Hindawi
Journal of Advanced Transportation
Volume 2021, Article ID 5642709, 20 pages
https://doi.org/10.1155/2021/5642709

Research Article

Multiscenario-Based Train Headway Analysis under Virtual Coupling System

Jinyi Pan,[1] **Qiyuan Peng**,[1,2,3] **Shuguang Zhan**,[1,2,3] **and Jiaqi Bai**[4]

[1]*School of Transportation and Logistics, Southwest Jiaotong University, Chengdu 611756, China*
[2]*National United Engineering Laboratory of Integrated and Intelligent Transportation, Southwest Jiaotong University, Chengdu, China*
[3]*National Engineering Laboratory of Integrated Transportation Big Data Application Technology, Southwest Jiaotong University, Chengdu, China*
[4]*Faculty of Geosciences and Environmental Engineering, Southwest Jiaotong University, Chengdu, China*

Correspondence should be addressed to Shuguang Zhan; shuguangzhan@my.swjtu.edu.cn

Received 10 May 2021; Revised 10 July 2021; Accepted 27 October 2021; Published 21 December 2021

Academic Editor: Luigi Dell'Olio

Chinese high-speed railway has implemented large-scale network operation with an urgent need for capacity improvement. The concept of virtual coupling seems to be a promising solution that provides a new operational scenario for high-speed railway, where trains are formed into a cooperative convoy and run synchronously with small train headways. The train-following principles under the virtual coupling signalling are quite different from those under conventional train control systems. Therefore, train headway analysis for different operational scenarios should be carried out to ensure railway safety and evaluate capacity benefits brought by virtual coupling. This paper proposes a potential virtual coupling architecture with reference to ETCS/ERTMS specifications. We compare blocking time models under different train control systems, and eight typical train-following scenarios are investigated for virtual coupling, including train arrival and departure cases. A detailed multiscenario-based train headway analysis is provided based on the microscopic infrastructure of the station and technological characteristics of virtual coupling. All computational outcomes are based on the train dynamic motion model. A comparative analysis of train headways under virtual coupling and CTCS-3 is provided in the case study. Results show that train headways can be substantially reduced under virtual coupling and are related to the station infrastructure layout.

1. Introduction

In China's high-speed railways, oversaturated utilization of capacity has become prominent with the increasing demand for high-density passenger services. There is an urgent need to obtain sufficient capacity gains and provide fast, convenient, and comfortable transport for the current large-scale networks [1]. One essential factor related to the capacity of a railway is the train headway, which refers to the minimum space or time interval that two trains must be separated. Hence, it is crucial to prevent trains from colliding or intruding into stations accidentally [2]. At stations, the interlocking area requires a train to travel at limited speeds when performing relevant services (e.g., arrival, departure, and passage of trains), and these station-related cases usually become the capacity bottleneck of a railway corridor [3]. The train control system extensively used in China, namely, CTCS-3, has implemented the quasimoving-block mode with a minimum train headway of 3 minutes. On-site feedback shows that under current operational conditions, the 3-minute target cannot be fully achieved. Upgrading system configurations and improving basic facilities are commonly adopted to address this issue [4], such as optimizing line conditions, adopting large size turnouts and sectional route release technology for stations, and improving the performance of rolling stocks. However, due to the high cost of reconstruction and maintenance, the effects of these measures are often overestimated. Shifting towards advanced signalling systems seems to be a more effective way [5], e.g., the communication-based train control system used in urban rail transit. The European Shift2Rail project was launched in July 2014. Its innovation programme 2 (i.e., advanced traffic management and control system) aims to utilize new technologies (e.g., satellite positioning, high-speed, high-capacity data, and automation) in train control systems to enhance traffic management [6]. As mentioned in innovation programme 2, virtual coupling (VC) could significantly reduce train headways and improve railway capacity. Institution of Railway Signal Engineers also pointed out that VC has great potential, but extensive exploration is required before it is put into use [7].

Under the conventional moving-block system (MBS), a train continuously receives the Movement Authority (MA) that indicates the maximum distance a train can cross in safe conditions from the Radio-Block Center (RBC). Building upon the real-time MA, the onboard computer can automatically calculate the braking curve that instructs the train to stop before reaching the danger point (i.e., the end of a preceding train or a movable track element). The corresponding absolute braking distance (i.e., the distance required for the train to brake to speed zero) increases dramatically with train speeds. For a high-speed train, the distance can even reach several kilometers [8]. Autonomous driving and cooperative platooning in road traffic theory provide a new operational idea for the railway market. A direct communication link can be established among trains, so that they can exchange information (i.e., speed profile, position, and train route/direction) with their neighbours, allowing every train to adjust its motion states in consideration of neighbouring trains. Therefore, two adjacent trains are allowed to be separated by a relative braking distance that takes into account the braking rates of different trains, rather than an absolute one [8]. In addition to massively reducing train headways, VC also implies a kind of flexible and intelligent train organization mode, which can better adapt to passenger/freight transport needs. A convoy (i.e., a train platoon separated by small headways running at coordinated speeds) can automatically decouple when approaching a junction or a station, and trains can also get virtually coupled at these locations or on the run. Before the convoy reaches the switch area where individual trains need to go to different routes (i.e., different railway lines or station tracks), an absolute braking distance and a safe margin should be maintained between the rear train and the switch area to ensure all the switches are set up safely.

A growing body of scientific projects such as X2Rail [9], Roll2Rail [10], and In2Rail [11] have been carried out to tackle technical problems (e.g., train control strategy, communication solutions, and system configurations) related to VC implementation. Train-following principles under VC signalling are quite different from those under conventional MBS or fixed-block system (FBS). Fundamental operational scenarios have been studied for VC signalling in the MovingRail project [12], combining different stopping patterns (train stopping or nonstopping) and typical train manoeuvres (i.e., plain line, merging junction, and diverging junction). Unlike other railway markets (e.g., main line and region), decoupling and coupling operations of high-speed railway trains are most likely to occur in station-related scenarios because trains run on a plain and independent line. From the perspective of operational safety, it is necessary to investigate the minimum train headway that must be satisfied for train manoeuvres in complex railway nodes, namely, high-speed railway stations. In addition, train headways are also essential for capacity evaluation and compilation of future train operation schedules based on VC.

When performing train-following simulations, some existing literatures ignore the station interlocking principle or detailed infrastructure data (e.g., train routes, track elements, and line-side signals) [13, 14]. With reference to the train headway calculation method reported in MovingRail deliverable [12], we address the train headway analysis in additional station-related scenarios from a microscopic perspective of the station layout. The specific configuration characteristics of VC signalling (e.g., system update time and communication delay) are considered and compared with conventional CTCS-3.

The remainder of this paper is organized as follows. Section 2 describes basic train control concepts and illustrates a CTCS-4-based VC structure. Section 3 reviews the related literature on VC from the perspectives of train control strategy and train organization. Section 4 analyses the application of the blocking time model in different train control systems and describes eight representative train-following scenarios. Section 5 details a train headway analysis for the eight train-following scenarios under VC. Section 6 reports the outcomes for train headways under VC system and CTCS-3 with a comparative analysis. Finally, conclusions and some preliminary hints for future research are presented in Section 7.

2. Train Control Concepts

2.1. CTCS Levels. CTCS (Chinese Train Control System) is constructed based on ETCS (European Train Control System) standards and adapted to China's specific transportation needs [15]. According to the functional requirements [16], CTCS is divided into five levels, of which CTCS-2 and CTCS-3 have come into common use in high-speed railways. The main operational characteristics of CTCS are shown in Table 1.

Before CTCS-3, data transmission from infrastructure to vehicles relies on the trackside devices, such as multi-information track circuits and controlled or uncontrolled transponders. However, the Global System for Mobile Communications (GSM-R) undertakes the bidirectional data transmission work in CTCS-3/4. Besides, the track clear detection no longer relies on the track circuits in CTCS-4 but RBC and onboard equipment (i.e., Train Integrity Monitoring System, Vehicle Onboard Controller (VOBC), and onboard sensors) [16]. Satellite-based train positioning is another feature of CTCS-4. In X2Rail-2 [17], it has been pointed out that train positioning could be achieved by equipment such as Virtual Balise Transmission System, with balises providing positioning reference for precision calibration.

Table 1: Characteristics of CTCS levels.

CTCS level	Blocking mode	Data transmission	Track clear detection
CTCS-0	Fixed-block	Trackside devices	Track circuits
CTCS-1	Quasimoving-block	Trackside devices	Track circuits
CTCS-2	Quasimoving-block	Trackside devices	Track circuits
CTCS-3	Quasimoving-block	GSM-R	Track circuits
CTCS-4	Moving-block or virtual-block	GSM-R	RBC and onboard equipment

2.2. Train Separation Principles. In railways, train movements are under the surveillance of train control systems to safely separate trains. Different train separation principles are illustrated in Figure 1 according to the characteristics of train control systems (see Table 1). Note that the virtual-block (i.e., block sections are virtually set by computers) mode under CTCS-4 can be regarded as a special quasi-moving-block, so it is not illustrated in Figure 1.

The train speed at the end of authority (Eoa) is v_{Eoa}. In FBS (see Figure 1(a)), railway lines are divided into continuous block sections. Whether a train can enter a section is governed by line-side signals or MA received on-board [15]. For instance, two following trains should be separated by at least four block sections on a railway with four-aspect signalling. In the quasimoving-block mode implemented under CTCS-3 (see Figure 1(b)), the RBC calculates the MA according to train speed and location information received from trackside devices, as well as the dispatching command received from the Dispatching Control Center. Then, the MA is issued to trains, enabling VOBC to compute the dynamic braking curve. The starting point of braking is the location where train safe braking can be ensured, but the Eoa is still the fixed boundary of a block section. A safety margin (s_m) is required between the danger point (i.e., the so-called supervised location) and Eoa under CTCS-4 and VC. In CTCS-4 (see Figure 1(c)), the fixed-block sections are removed and trains are separated by an absolute braking distance plus a s_m. Note that due to the excessively long braking distance, a full MBS may not bring satisfactory capacity gains for high-speed railways versus conventional FBS. Under VC signalling, trains do not have to stop in front of the Eoa (see Figure 1(d)). Benefited from the robust and fast communication link between trains, a train can not only calculate the braking curve according to its motion states but also take into account the real-time information received from neighbouring trains. Thus, the interval between consecutive trains can be reduced to a considerably short distance (i.e., a relative braking distance plus a s_m). For high-speed railways, the s_m under VC operation is recommended to be 50 to 200 m in MovingRail [18].

2.3. Structure of VC System. VC system is a train-centric signalling system. There is currently no standard specification for the VC architecture. Figure 2 shows a potential structure of VC. The distinction between VC and CTCS-4 is the addition of a vehicle-to-vehicle communication link (i.e., the V2V layer). Centralized Traffic Control (CTC) is responsible for monitoring train movements and delivering operation instructions (e.g., train operation schedules and dispatching commands) based on the operational requirements of VC. Computer-based interlocking (CBI) can handle the station-related routes (i.e., arrival, departure, and shunting routes) after checking and confirming some essential issues, e.g., states of train motions and trackside devices. RBC operates as a virtual leader during VC operations; it calculates basic MA that indicates the last safe point for the convoy. It is worth noticing that the deployment of the V2V layer will lead to a more complex control mechanism when compared with CTCS-4, as the contents of MA are enriched with real-time motion states (i.e., objective route and speed profiles) from nearby trains. Moreover, trains are equipped with Automatic Train Operation (ATO) to achieve automatically driving. In terms of the communication solution of the V2V layer, MovingRail [19] outlined that 5G principles are suitable which also conform to the development trend of the Future Rail Mobile Communications System. Necessary elements (e.g., antenna, transmitter, and receivers) are required to be installed on vehicles.

3. Literature Review on Virtual Coupling

VC technology was mainly studied for freight transport in the early bibliography [20, 21]. Bock et al. [20, 21] first proposed VC concept: the mechanical connections between vehicles are cancelled and every vehicle has its power device and control computer. In [22, 23], the preliminary facilities and basic concepts of VC were further addressed. In recent years, VC has been gradually recognized as an attractive technology for passenger transport. Goikoetxea [24] mentioned that the complete implementation of VC relies on the onboard configurations, new functions, and upgrade functionalities. The Shift2Rail project was established under Horizon 2020 and aims at achieving the most sustainable, cost-efficient, high-performing, time-driven, digital, and competitive customer-centred transport mode for the European railway [6]. Well-directed researches have been conducted on VC technology within the Shift2Rail initiative, covering system required technologies (e.g., new traction technology, satellite positioning, communication solution, and security) and feasibility analysis from the perspectives of operation, technology, and business [6]. In this section, we review the state of the art from two aspects: train control strategy and train organization theory under VC.

3.1. Review of Train Control Strategies. Advanced train control systems ensure that trains operate as scheduled based on the original timetable [25]. In terms of train control under MBS, Pan et al. [26] adopted the theory of Multiagent Systems (MAS) to establish railway elements (e.g., trains and

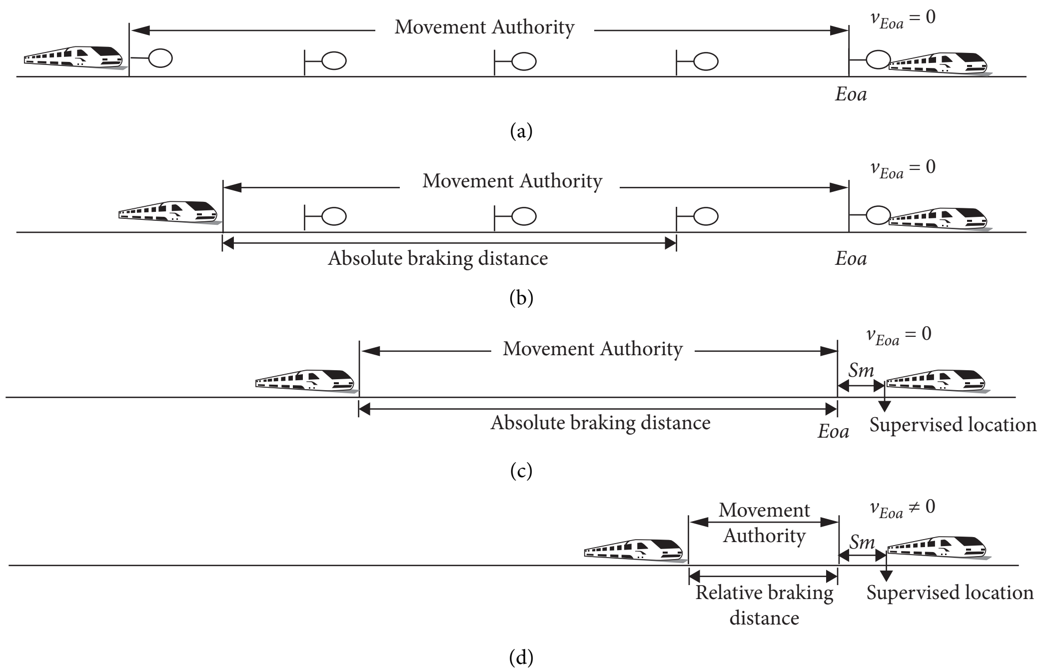

FIGURE 1: Typical train separation principles. (a) Fixed-block. (b) Quasimoving-block. (c) Moving-block. (d) Virtual coupling.

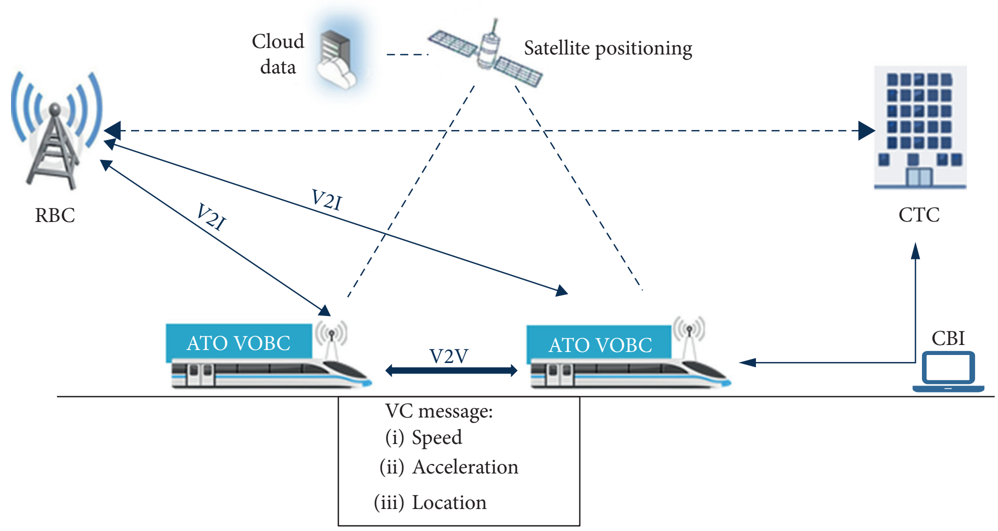

FIGURE 2: A potential system architecture of VC in the future.

stations) as intelligent subject models. Solutions were further proposed in response to train integrity detection, train mobility management technology, and coordinated train control mechanism. Ning et al. [27] proposed a distributed cooperative control method for high-speed trains, and the target was to maintain the minimum tracking distance between trains. Gao et al. [28] studied the cooperative prescribed performance tracking control problem for multiple high-speed trains. Train speed and position were supervised by Automatic Train Protection (ATP) and MA at any instant. Note that the speed information of adjacent trains is not considered in the control strategies for MBS and trains are separated by absolute braking distance (i.e., "hit-hard-wall" mode).

Cooperative driving allows trains to group into a virtually coupled platoon on the run or at a standstill. Different control strategies have been mentioned in numerous studies, and usually, the operation goals are maintaining an expected following distance between trains and all trains cooperatively move forward at optimal velocities (i.e., the acceleration or deceleration status of trains in a convoy is synchronized). Di Meo et al. [29] pointed out that appropriate mathematical models and control algorithms borrowed from the automotive field can prove the effectiveness of cooperative control strategies under VC. Liu et al. [30] established a coordinated control model in which trains could adjust their motion states according to different train tracking strategies. Liu [14] proposed a dual-aspect train control algorithm that could coordinate the speed and following distance of trains concerning the car-following theory on road traffic. The parameter value in a train-following formula was demonstrated to be critical for system stability. Liu et al. [31] considered train operation safety, passenger comfort, and train punctuality to obtain an optimal train control strategy. Felez et al. [32] utilized a decentralized model predictive control (MPC) framework to control trains in a platoon; they also proved that VC could greatly shorten the train headway and ensure the safe separation of trains.

3.2. Review of Train Organization under VC System. VC is also known as a dynamic formation method. Shorter grouping trains and more frequent train services will better meet flexible travel demands [18]. Train control and dispatching organizations should be well integrated to ensure safe operation and maximize the potential of VC. Liu et al. [33] proposed a spatial-temporal dispatching method that was adaptable for real-time passenger flow based on VC. Preliminary operational characteristics (e.g., train compositions, onboard customer facilities, train platforming and crowd management, power supply, and convoy control) corresponding to different railway markets were investigated in MovingRail [18]. Compared with other markets, the regional and freight markets may be more interested in VC because they urgently need to increase the current train frequency despite the expensive reconstruction and operating costs [34]. For high-speed railways with high-density passenger services, VC can also bring huge capacity growth to some potential cases, e.g., trains consecutively overtaking at a station, passing through a junction or a station. The German Aerospace Center [35] has integrated the VC technology into the study of the next-generation train and developed dedicated simulation software for trains operating under VC. Based on this simulation tool, Schumann [13] explored VC-related scenarios with conventional switches and passive switches. The simulation results on the Shinkansen high-speed line showed the benefits of VC, especially when trains in a convoy continuously performed stopping or departing services at stations. Quaglietta et al. [8] proposed a specific MA content under VC signalling and the form of message exchanged via the V2V communication layer. A multistate train-following model was also developed to investigate capacity gain in train stopping cases and diverging junction cases. To calculate headways of trains departing from a station under MBS, Mei et al. [36] introduced a calculation method based on geometric progression. Three cases were depicted: two stationary trains departed consecutively, the preceding train passed through the station, and the rear departed from the station, and two trains successively passed through the station. Liu et al. [37] proposed a VC-based station dispatching method by dividing train operation routes into segments and switches could be continuously locked for virtually coupled trains. In this article (i.e., train headway analysis in hereinafter), we also assume that switches in the interlocking area can be continuously locked for multiple trains that occupy the same operation route in the station.

From the state of the art, VC is technically feasible, but in terms of its implementation in the railway field, it is still in the experimental stage. The definition of the train-following principle in station-related operational scenarios is not yet clear for VC signalling. This paper aims at obtaining an in-depth train headway analysis of representative operational scenarios concerning the characteristics of VC as well as operational requirements in current high-speed railways.

4. Train-Following Analysis under VC System

4.1. Blocking Time Model. The minimum headway between two consecutive trains depends on the so-called "blocking time." It is the needed time for a train to cross the section that is allocated exclusively to this train and blocked to others [38]. The blocking time model is applicable for FBS but needs to be modified for MBS and VC. Quaglietta et al. [39] first elaborated the blocking time model adapted to VC. We refer to the blocking time model [39] to further analyze the train headways in station-related scenarios. The basic blocking times are as follows [15]:

(1) Time required for clearing the signal
(2) Signal watching time and reaction time
(3) Approaching time
(4) Time for passing the block section
(5) Time for completely clearing the block section and the track circuit overlap
(6) Time for releasing the block section

For China's conventional lines in which trains are governed by line-side signals, the approaching time refers to the time needed to cross the previous block section (i.e., the distance between section signals at both ends). For FBS with cab signals, the approaching time is the time needed to cross the absolute braking distance based on the supervision curves. The signal watching time is no longer needed in this case, but the rest time components are consistent with the former.

When trains run in the switch section (i.e., station or junction) under MBS or VC system, since there is no passive switch available, the block-related time (i.e., time for passing, clearing, releasing the block section, and signal clearing time) is still required. However, these times do not exist when trains run on the main line. A train operating under MBS must be at a standstill before reaching Eoa, so the approaching time refers to the travel time of an absolute braking distance. For trains operating under VC system, the approaching time represents the time needed for a rear train to coordinate to the preceding train speed [39]. Also, the reaction time under VC signalling is much shorter than that under other systems due to the application of ATO.

4.2. Description of Train-Following Manoeuvres under VC System. Due to the speed limit near the switch area, VC operation can be initiated in the two most likely cases: trains departing from a station or trains from different directions merging into the same route at a junction. Similarly, for the cases in which a convoy is approaching a station, or train routes diverge at a junction, the decoupling of trains can be initiated. The newly constructed high-speed railways in China are independent lines with homogeneous rolling stocks. Therefore, in this paper, we focus on the station-related train-following manoeuvres and do not consider the junction-related scenarios. The actual forces on trains change continuously with train movements and trains are not always traveling at constant speeds. Before carrying out train headway computations, we furthermore consider the following assumptions:

(1) The traction acceleration rate of trains with a certain type of EMU is constant.

(2) The braking deceleration rate is considered as a piecewise constant function which is related to the actual train speed.

(3) The basic resistance generated by several types of friction and aerodynamic resistance are considered in the computation. The additional resistances caused by tunnels, ramps, and curves are ignored in the station-related scenarios.

(4) Virtually coupled trains cannot stop at the same platform.

(5) For the train arrival cases (scenarios 3, 4, and 5) under VC signalling, when the preceding train clears all critical elements of the interlocking area, the following train has already slowed down to a relatively low speed.

Table 2 depicts eight train-following manoeuvres that may occur during train operations. For the sake of clarity, only two trains are shown. Scenarios 1 and 2 refer to a convoy running on the main line and passing through a station consecutively, respectively. Three arriving manoeuvres are designated as scenarios 3, 4, and 5, and trains can get decoupled if they are arranged to different station routes. In scenario 3, two virtually coupled trains are required to stop on different tracks at the approaching station. In scenario 4, the preceding train G1 passes through the station without stopping, and the rear G3 needs to stop. In scenario 5, the preceding train G1 needs to stop, and the rear G3 instead passes through the station. In the train departure cases, we envisage that trains are scheduled to form a convoy after leaving the station and gradually reach the virtually coupled state during operation. In scenario 6, two stationary trains G1 and G3 from different tracks both leave the station. In scenario 7, G3 must wait for G1 to pass the station before leaving. In scenario 8, G3 must wait for G1 to leave before it can pass through the station.

5. Analysis of Multiscenario-Based Train Headway under VC System

5.1. Route Releasing in Station-Related Scenarios. In the station interlocking area where switch occupancy occurs frequently, train-following must comply with interlocking principles. Therefore, in terms of the station-related scenarios, train headway analysis should be carried out based on the blocking time model mentioned in Section 4.1. For the station routes corresponding to two trains, the switches that need to be occupied by both trains are called associated switches. A sectional route release mode is considered for station automatic route releasing, which means that as long as the last critical track element (i.e., the track circuit where the last associated switch is located) is completely cleared by the preceding train, the route for the rear train can be unlocked. Figure 3 depicts an example of two trains entering different station tracks: the target track of G1 is track 1, and the rear G3 can either stop on track 2 (see Figure 3(a)) or track 3 (see Figure 3(b)). The receiving route from the station home signal to the last critical track element (referred to as the clearing point in Figure 3) is shown by the red line. We find that the route length in track combination 2 is shorter than that in track combination 1 due to the difference in the position of the clearing point. Therefore, we can conclude that the sequences of track usage will affect the position of the clearing point and further affect the timing of unlocking the receiving route for the rear train. For trains departing from different station tracks, we consider that switches can be continuously locked for trains which share the same route (i.e., the continuous track circuits that are occupied by multiple trains).

5.2. Train Headway Analysis under Eight Operational Scenarios

5.2.1. Scenario 1: Trains Running on the Main Line. When trains run on the main line under CTCS-3, the minimum required distance between two consecutive trains includes the absolute braking distance of the rear train, the block section length, the train length, and a safety margin before the block section. Figure 4 depicts the basic train-following case in which trains run cooperatively on the main line under VC. The two trains are the preceding train $i-1$ (the leading train) and rear train i (the following train). Ideally, trains in the rear can follow the leading train with desired space intervals and coordinated speeds.

Since cooperative driving strategies have been extensively studied in previous literature, we adopt the following formulas from Di Meo et al.'s study [29] to denote the objects of VC:

$$l_i(t) \longrightarrow l_{i-1}(t) + L^{de\,s}(t) \quad v_i(t) \longrightarrow v_{i-1}(t) \quad a_i(t) \longrightarrow a_{i-1}(t),$$
$$L^{de\,s}(t) = l^{st}_{i,i-1}(t) + Tv_{i-1}(t), \tag{1}$$

Table 2: Train manoeuvre scenarios under VC system.

Trains consecutively running

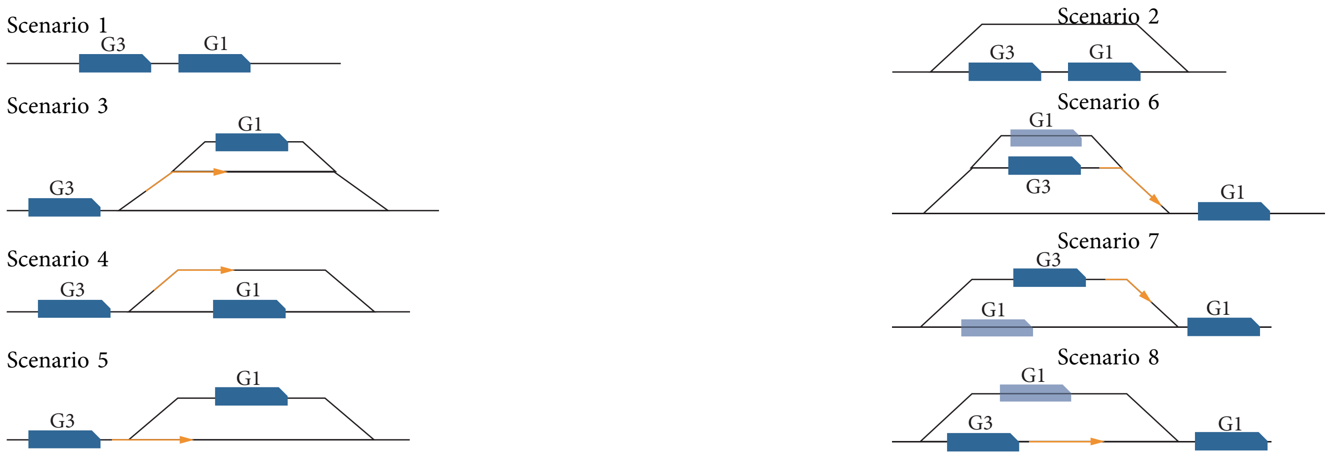

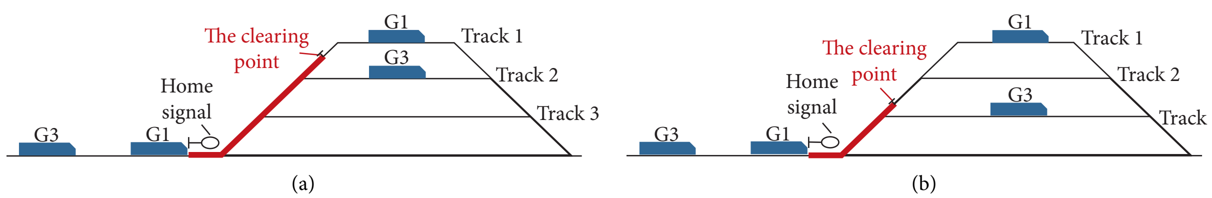

Figure 3: Positions of the clearing points corresponding to track combinations 1 and 2. (a) Track combination 1. (b) Track combination 2.

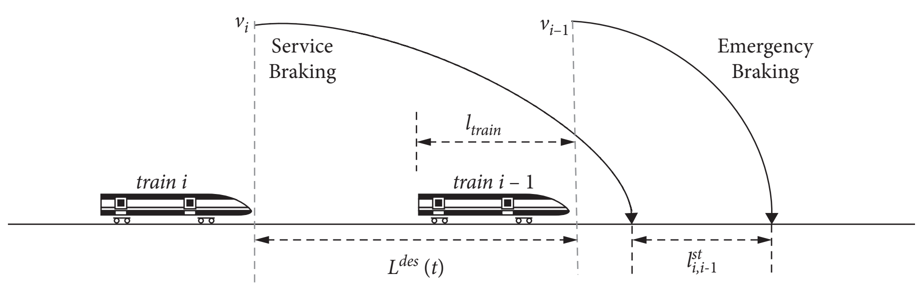

Figure 4: Trains simultaneously running in sections.

where $l(t)$, $v(t)$, and $a(t)$ are the train position, speed, and acceleration, respectively. $L^{de\,s}(t)$ is the desired following distance between consecutive trains which can be calculated by equation (1). According to the spacing policy [40], $l^{st}_{i,i-1}$ represents the minimum required distance between trains at a standstill, T is the desired time headway, and the value of T cannot be less than a critical value [41]. Both $l^{st}_{i,i-1}$ and T are set as constant controlling parameters [29].

5.2.2. Scenario 2: Trains Consecutively Passing through a Station. The route handling procedure is required for every train passing through a station under CTCS-3. Generally, two block sections ahead must be cleared before the station home signal indicates a clear aspect (i.e., a train may proceed) for a train. The required distance between trains equals the train absolute braking distance plus the total length of block sections ahead. Moreover, a certain time for train passing operations (i.e., sight and reaction, transferring track circuits states, and clearing the signal) should be considered. However, the route handling procedure is only required for the leading train when a convoy runs under VC. Trains in a convoy can consecutively pass through the station with small intervals. Therefore, the train headway in scenario 2 is the same as that in scenario 1. It is no doubt that the train organization pattern in scenario 2 can significantly increase the number of trains passing the station per unit time.

5.2.3. Scenario 3: Trains Arriving at a Station. The blocking time in the train arriving case under CTCS-3 includes train approaching time (i.e., time needed to decelerate from train maximum speed to the station allowable speed), time needed to clear the critical elements in the station interlocking area, and time for train arriving operation (i.e., setting switches in correct positions, sight and reaction, transferring track circuits states, and clearing the home signal).

The main difference of the blocking time in the VC case is that the approaching time is much shorter than that in CTCS-3. In addition, the reaction time is reduced thanks to the ATO. As illustrated in Figure 5, G1 and G3 both need to perform stopping services at the approaching station. Virtually coupled trains can get decoupled because they are assigned to different station tracks. The respective target tracks of G1 and G3 have been marked in Figure 5. The blue and orange solid lines represent the relative motion states of G1 and G3, and the orange dashed line represents the braking curve of G3. The upper and lower parts of Figure 5 show the changes in train distance and speed and the changes in train distance and time, respectively. The train headway can be obtained by adding up each part of the blocking times.

The virtually coupled trains slowdown in advance to not exceed the station allowable speed. G3 must wait for G1 to completely clear all critical track elements of the interlocking area before entering the station. The clearing point here is the end of the track circuit where the last associated switch (i.e., switch 5) is located. When G1 crosses the clearing point, there are some essential operations (referred to as the arrival operation in Figure 5) required before initiating the receiving procedure of G3, i.e., setting switches in correct positions, ATO reaction, transferring track circuits states, and clearing the home signal. To prevent G3 colliding with the station, an absolute braking distance of G3 and a station safety margin should also be maintained between G3 and the home signal. Note that the station safety margin s_m here refers to the reserved distance to protect the home signal. The time needed to cross the absolute braking distance is called the approaching time of G3. The calculation formula of train headway in scenario 3 can be expressed as

$$I = T_{\text{arr}} + \frac{l_{b3}}{v_3} + \frac{s_m + l_{\text{enter}} + l_{\text{train}}}{v_1}, \tag{2}$$

where T_{arr} represents the arrival operation time, which is determined by system configurations. l_{b3} is the absolute braking distance when train G3 applies service braking. v_3 is the speed of G3, which is an indeterminate value, and cannot be greater than the allowable speed v_{lim} when G3 reaches the Eoa. s_m is the station safety margin in front of the home signal and l_{train} is the train length. l_{enter} represents the distance from the home signal to the clearing point. Before reaching the clearing point, G1 may run at a constant speed v_{lim} or run at a uniform speed and then decelerate. l_{c1} and $l_{b1}^{'}$ represent the distance travelled by G1 at a constant speed v_{lim} and the deceleration distance; we can obtain $l_{c1} + l_{b1}^{'} = l_{\text{train}} + l_{\text{enter}}$. v_1 is the speed of G1, which depends on the actual dynamics of the train during the entire process.

5.2.4. Scenario 4: The Preceding Train Passes through the Station and the Rear Stops. In scenario 4, the preceding train passes without stopping but the following train needs to stop. For both CTCS-3 and VC cases in scenario 4, the train arriving operation time and approaching time are the same as those in scenario 3. The times for a preceding train to clear critical track elements are different because the clearing point here is the opposite exit signal (i.e., the signal that instructs the train in the opposite direction to exit the station). As depicted in Figure 6, the preceding train G1 passes the station at its original speed v_m, and G3 needs to stop at the station. Two virtually coupled trains can get decoupled and the movement of G1 will not be affected. Before G3 can enter the station, the preceding train should have entirely crossed the opposite exit signal and the train arriving operations (i.e., transferring track circuits states, setting switches in correct positions, clearing the home signal, and ATO reaction) should have been completed. Moreover, a station safe margin and an absolute braking distance of G3 should be maintained between G3 and the home signal.

The train headway calculation method for scenario 4 is similar to equation (2), but l_{enter} is the distance between the station home signal and the opposite exit signal on the main track. v_1 is the original speed of G1, because G1 does not need to stop but pass with a high speed.

5.2.5. Scenario 5: The Preceding Train Stops and the Rear Passes through the Station. In scenario 5, the preceding train needs to stop and the rear one passes without stopping. For both CTCS-3 and VC cases in scenario 5, the times for clearing critical track elements are the same as those in scenario 3. In addition, the times for train passing operation are needed. For CTCS-3, the train approaching time equals the time for the rear train to cross the absolute braking distance (i.e., distance needed to decelerate from the original speed to zero) at its original speed. As illustrated in Figure 7, the two virtual coupled trains both need to slowdown before arriving. After G1 completely crosses the clearing point (i.e., the end of the track circuit where switch 1 is located), G3 can accelerate and pass the station.

The calculation formula of train headway is similar to equation (2), and the difference lies in the motion states of train G3. In scenario 5, G3 should accelerate rather than decelerate to pass the absolute braking distance. The passing operation here includes the following components: transferring track circuits states, setting switches in correct positions, clearing the home signal, and ATO reaction. According to the current CTCS-3 operational standard, the time for passing operation is shorter than the arrival operation time in scenarios 3 and 4.

5.2.6. Scenario 6: Two Stationary Trains Departing from the Station. The monitoring mode under CTCS-3 requires that only when the train in front has cleared the first exit block section, the rear one can start. The first exit block section refers to the block section behind the opposite home signal (i.e., the signal that instructs the train in the opposite direction to enter the station). Therefore, the blocking times in the train departure case under CTCS-3 contain the following components: time for the preceding train to cross the distance between the train parking sign and the end of the first

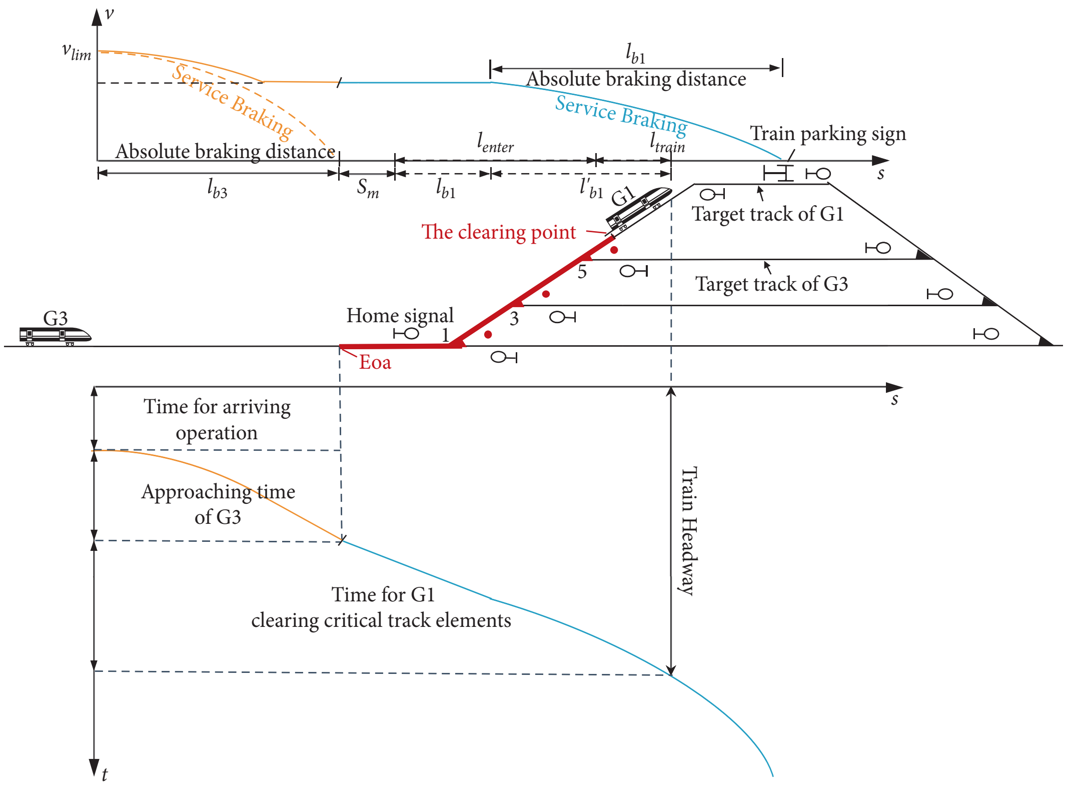

Figure 5: G1 and G3 both arrive at a station.

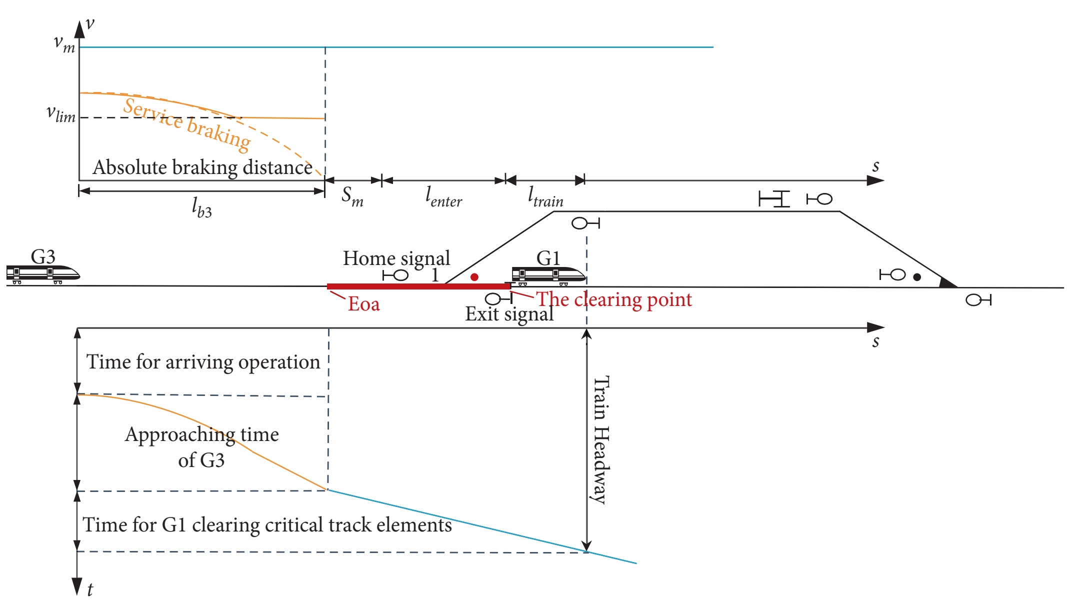

Figure 6: G1 passes through the station and G3 arrives at the station.

exit block section and time for train departure operation (i.e., sight and reaction, transferring track circuits states, setting switches in correct positions, and clearing signals). The length of the first exit block section should not be less than the distance required for the train to decelerate to a standstill at the station's allowable speed, which is considerably long for high-speed railway stations. Figure 8 describes the departure operations of G1 and G3 under VC. The corresponding train headway has a great influence on the composition of the train convoy.

G1 and G3 start from different tracks and both arrive at the main line. There is a common route that will be occupied by both trains (e.g., switch 4 and switch 2 in Figure 8). Hence, the clearing point here is the first critical element

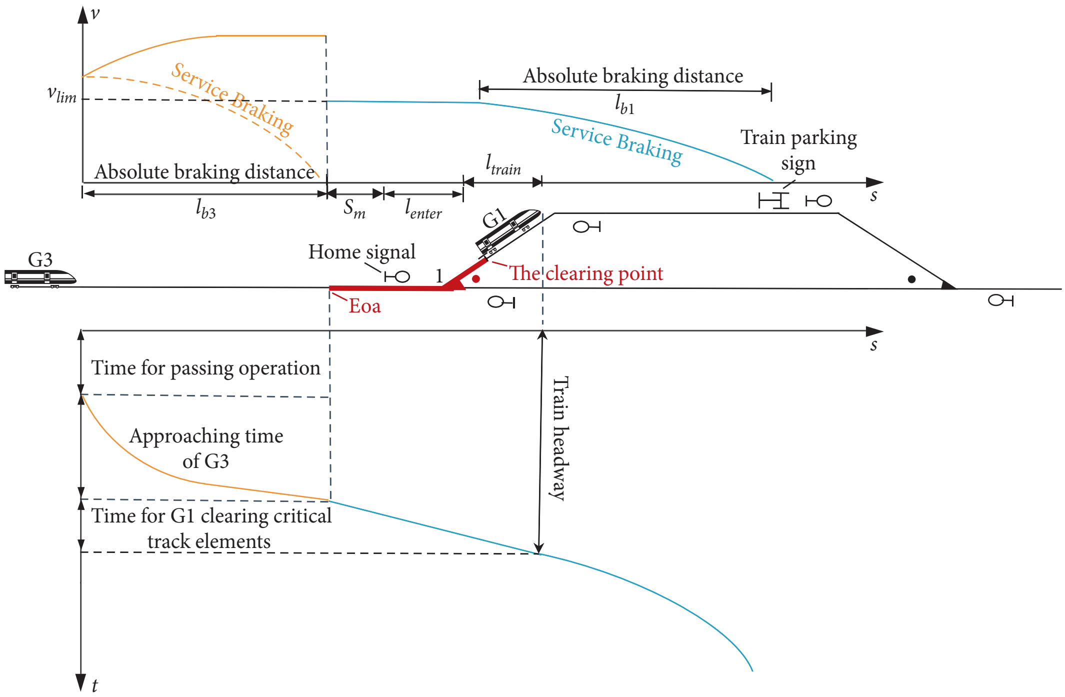

FIGURE 7: G1 arrives at the station and G3 passes through the station.

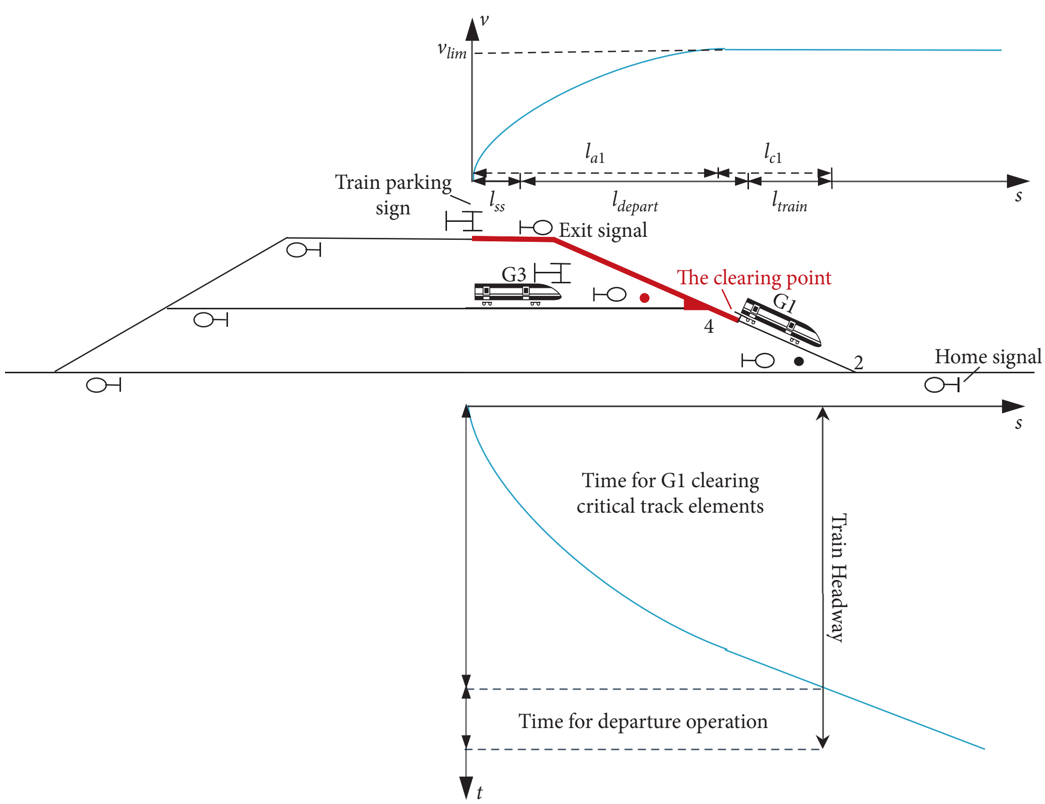

FIGURE 8: G1 and G3 both depart from the station.

(i.e., the end of the track circuit where switch 4 is located) because the route behind this point is the same for G1 and G3. Benefiting from the V2V communication layer, G1 and G3 can continuously exchange position, speed, and acceleration information. Therefore, once G1 has crossed the clearing point, G3 can depart after a certain time for departure operation (i.e., ATO reaction time, time for clearing the exit signal, setting switches in correct positions, and transferring track circuits states). Note that only the first critical switch needs to be reset for G3. The headway formula in scenario 6 can be written as

$$I = \frac{l_{ss} + l_{\text{depart}} + l_{\text{train}}}{v_1} + T_{\text{dep}}. \quad (3)$$

Here, l_{ss} represents the distance between the train parking sign and the exit signal on the track. l_{depart} is the distance from the exit signal to the clearing point. l_{train} is the length of G1. v_1 is the speed of G1, which changes dynamically during the departure process. G1 first accelerates to the turnout speed and then runs at this constant speed until leaving the station. The actual running distance of G1 at the station may be an entire acceleration distance or consists of acceleration distance l_{a1} and uniform speed distance l_{c1}. We can obtain $l_{ss} + l_{\text{depart}} + l_{\text{train}} = l_{a1} + l_{c1}$. T_{dep} refers to departure operation time.

5.2.7. Scenario 7: The Preceding Train Passes through the Station and the Rear Departs. Scenario 7 refers to the case in which the preceding train passes the station and the rear starts from a standstill. For CTCS-3, the preceding train should clear the first exit block section at its original speed. The time needed for train departure operation is the same as that in scenario 6.

As illustrated in Figure 9, the clearing point in scenario 7 is the opposite home signal, which means when G1 has crossed the signal, the departure procedure of G3 can be handled after essential departure operations. The calculation equation of train headway in scenario 7 is similar to equation (3). Note that $l_{de\ part}$ is the distance between the train parking sign and the opposite home signal. v_1 is the constant full speed v_m of G1.

5.2.8. Scenario 8: The Preceding Train Departs and the Rear Passes through the Station. For the CTCS-3 case in which the preceding train departs from a standstill and then the rear passes the station, after the preceding train leaves the first exit block section, it should continue to accelerate to reach the rear train's speed. Therefore, the time that the preceding train continues to accelerate should be added to the blocking times. For the VC case illustrated in Figure 10, the preceding train G1 first starts from a standstill and accelerates to the train allowable speed. G1 continues to accelerate to G3's speed after crossing the opposite home signal. Therefore, the additional acceleration time should also be considered in the train headway under VC.

The calculation formula of train headway can be expressed as follows:

$$I = \frac{l_{ss} + l_{\text{depart}} + l_{\text{train}} + l_{a1}'}{v_1} + T_{\text{pass}}, \quad (4)$$

where the definitions of l_{ss}, l_{depart}, and l_{train} are the same as those in equation (3). l_{a1}' represents the distance for G1 to accelerate to G3's speed. v_1 represents the dynamic speed of G1 during the entire process. T_{pass} is the passing operation time corresponding to scenario 8. While G1 is accelerating after clearing the opposite home signal, the station can prepare the passing procedure for G3 at the same time. Therefore, there is an overlap time for route handling (i.e., setting switches in correct positions and transferring track circuit states) that should be deleted.

6. Case Study

In the train-following scenarios introduced in Section 5.2, the calculation of the blocking times involved in equations (2)–(4) are established on the train traction calculation method [42]. We detail the dynamic motion model for high-speed trains in Appendix A. According to the decelerations and accelerations corresponding to different speed levels, the train distance and travel time within a certain speed range can be obtained. All relevant calculations (e.g., train speed, distance, and running time) are implemented in C++. The results will be compared with the train headway under CTCS-3 as we aim at estimating the capacity gain brought by VC technology. Besides, impacts from station infrastructure layout and some operational parameters can also be demonstrated. Tian et al. (2015) referred that railway capacity and operation efficiency are greatly limited by two types of station-related headways: train arrival headway (corresponding to scenario 3) and train departure headway (corresponding to scenario 6). The comparative analysis will focus on these two cases, but we also report the train headways of other station-related scenarios in Appendix B.

6.1. Experiment Setting. We choose Shanghai-Hongqiao Station in China as an example and assume that VC signalling has been embedded in the Beijing-Shanghai high-speed railway. Trains are scheduled to perform arriving/departing services at Shanghai-Hongqiao Station. All relevant calculation data (e.g., the length of the departure/receiving route, positions of track elements, train speed, and turnout speed) are on-site data from Shanghai-Hongqiao Station. Figure 11 depicts the infrastructure layout of the high-speed yard in the station, which also marked the number of the switch and the locations of main signals.

There are a total of 19 tracks in the high-speed yard. Tracks 1–14 can receive downward trains. Tracks IX and *X* are the downward and upward main lines, respectively. Tracks 1–19 can receive upward trains and send out trains in both directions. We study the train arrival headway and the train departure headway for the downward trains and upward trains, respectively. Table 3 shows the basic information of train routes, the target track, and the start track corresponding to train arrival and departure manoeuvres. The start and end corresponding to each train route are represented by start and end signals, respectively. In terms of train arrival case, the route starts from the home signal *X* on the main line and ends with the exit signal on the target track, while for the train departure case, the route starts from the exit signal on the start track and ends with the opposite home signal XN. Note that there may be more than one train

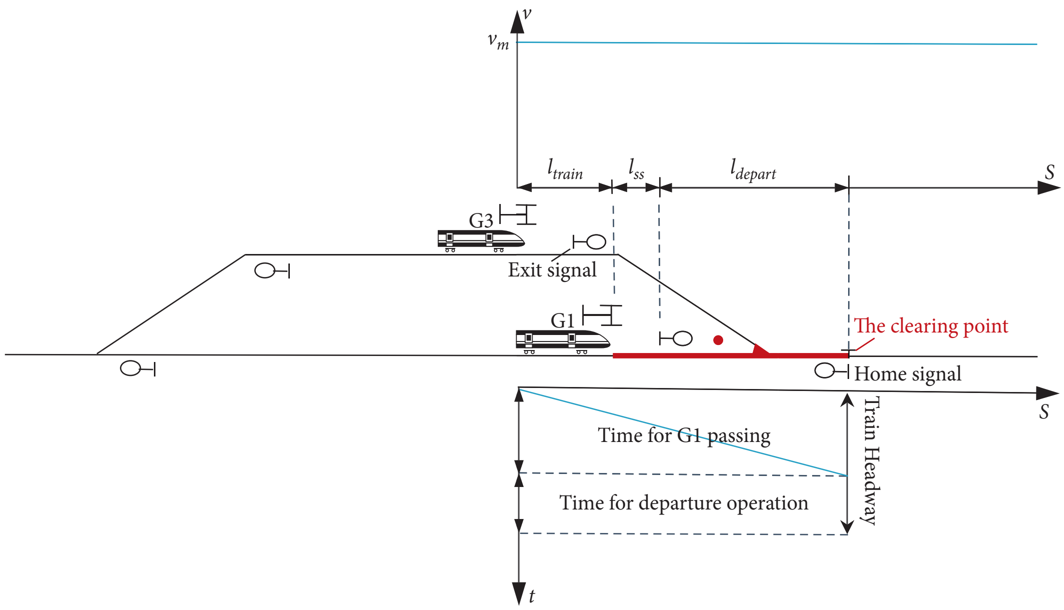

Figure 9: G1 passes through and the rear G3 departs from the station.

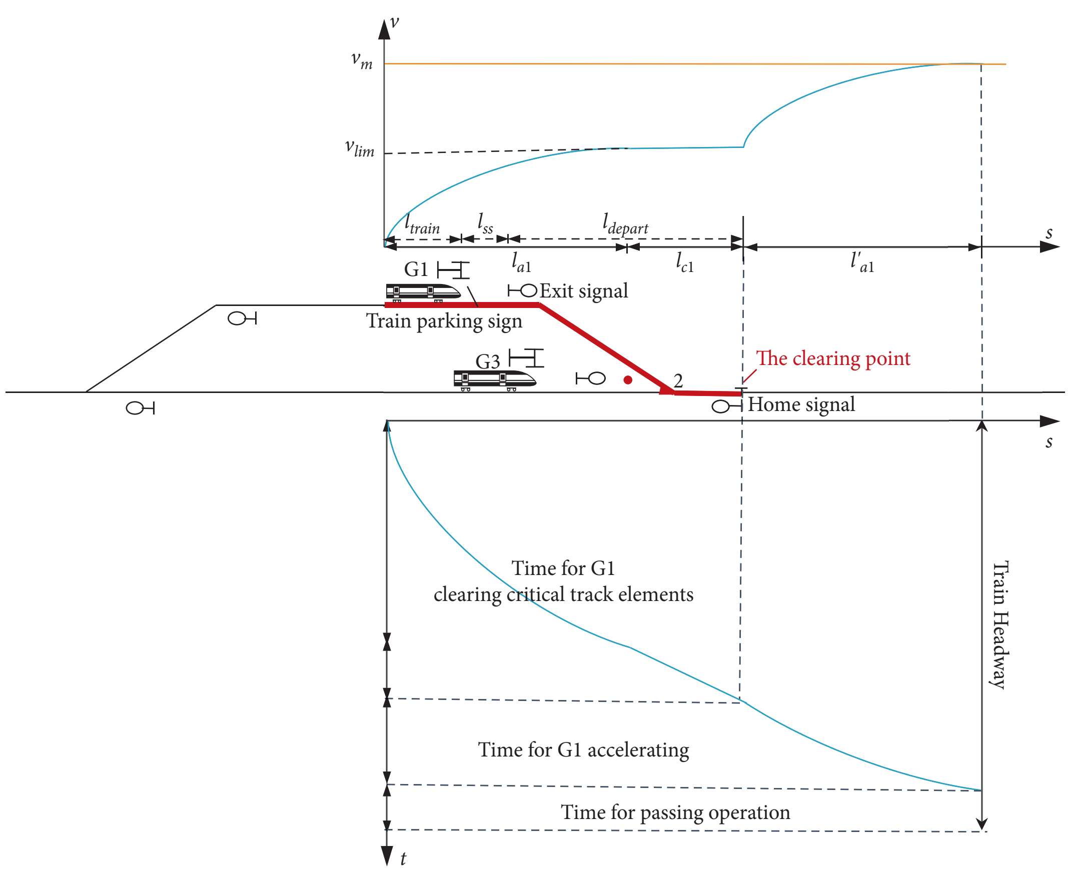

Figure 10: G1 departs and G3 passes through the station.

routes corresponding to each track, but we only selected one route for calculation. The length of each route is obtained by adding the lengths of all relevant track circuits.

The commonly used EMUs in China is the 8-vehicle train with a length of about 200 m or the 16-vehicle train with a length of about 400 m. We take CRH380BL as the

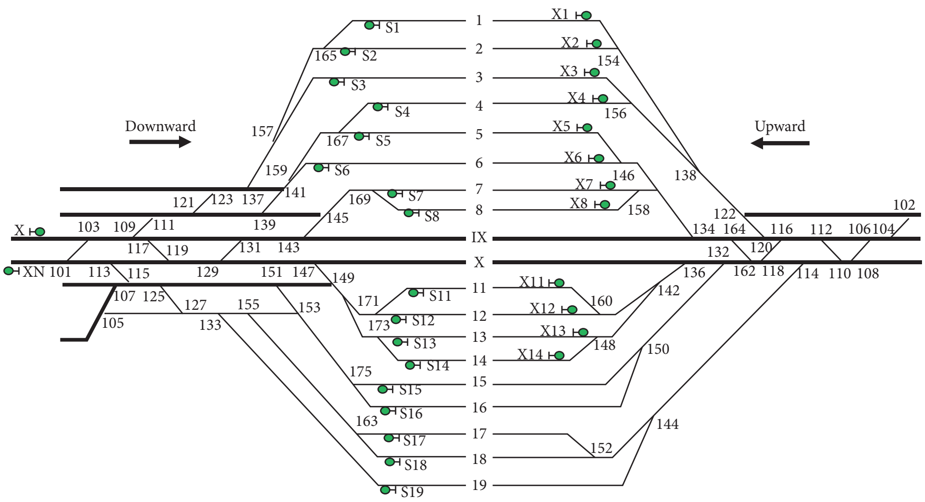

Figure 11: High-speed yard infrastructure layout of Shanghai-Hongqiao Station.

Table 3: Station route information of the high-speed yard in Shanghai-Hongqiao Station.

	Arrival route of downward trains				Departure route of upward trains		
Target track	Start signal	End signal	Route length [m]	Start track	Start signal	End signal	Route length [m]
1	X	X1	1963	1	S1	XN	1300
2	X	X2	1963	2	S2	XN	1300
3	X	X3	1951	3	S3	XN	1225
4	X	X4	1951	4	S4	XN	1308
5	X	X5	1983	5	S5	XN	1308
6	X	X6	1983	6	S6	XN	1219
7	X	X7	1916	7	S7	XN	1355
8	X	X8	1916	8	S8	XN	1355
11	X	X11	1916	11	S11	XN	1322
12	X	X12	1916	12	S12	XN	1322
13	X	X13	1983	13	S13	XN	1318
14	X	X14	1983	14	S14	XN	1318
				15	S15	XN	1324
				16	S16	XN	1324
				17	S17	XN	1278
				18	S18	XN	1278
				19	S19	XN	964

calculation object, which is formed of 8 motor vehicles and 8 trailers with a length of 399.27 m. The standard CRH380BL is equipped with an onboard ATP named CTCS3-300T. The service braking (SB) and emergency braking (EB) parameters are shown in Table 4.

The calculation results corresponding to different speed ranges are obtained by the train dynamic combined with the deceleration values in Table 4. Several calculation results at different initial and final speeds for CRH380BL are shown in Table 5.

Arrival operation time T_{arr} and departure operation time T_{dep} are necessary components of the train headway. The necessary time for arrival operation and departure operation includes reaction time, releasing time, turnout switching time, and signal clearing time. The reaction time is shorter than that in conventional CTCS-3, but the system delay time of the V2V communication layer should be considered. The rest time components of T_{arr} remain unchanged. According to the previous study [2] about train headway in current CTCS-3 and state-of-the-art research about VC deployment [36], we define the scenario-related parameters in Table 6. The parameters k, m, and n in Table 6 are empirical parameters used in the train dynamic motion model (see Appendix A).

6.2. Comparative Analysis of Train Headways

6.2.1. Train Headway in Train Arrival Case. For the train arrival case (scenario 3) under VC, we suppose that when the preceding train clears all critical elements of the interlocking area, the following train has already slowed down to the station allowable speed (i.e., 80 km/h). Therefore, the latter can cross the absolute braking distance at constant speed. In fact, before trains arrive at the station, the speed of the following train depends on the cooperative control strategy

Table 4: ATP parameters of CRH380BL.

EMU	Speed level [km/h]	Deceleration [m/s^2]	Acceleration [m/s^2]
CRH380BL (SB)	$0 \leq v \leq 125$	−0.68	0.4
	$125 < v \leq 160$	−0.59	
	$160 < v < = 200$	−0.53	
	$200 < v < = 240$	−0.48	
	$240 < v < = 280$	−0.44	
	$280 < v < = 325$	−0.39	
CRH380BL (EB)	$0 \leq v \leq 100$	−0.81	
	$100 < v \leq 140$	−0.68	
	$140 < v < = 180$	−0.59	
	$180 < v < = 220$	−0.53	
	$220 < v < = 260$	−0.49	
	$260 < v < = 325$	−0.46	

Table 5: Computation results at different initial and final speeds.

Initial speed [km/h]	Final speed [km/h]	Distance [m]	Time [s]
300	80	5737	105
80	0	357	32
0	80	634	57
80	300	9741	179

Table 6: Scenario-related parameters for CTCS-3 and VC system.

Scenario-related parameter	Value
k	0.000103
m	0.0066
n	0.42
Length of the first exit block section	1045 m
Max train speed	300 km/h
Station safety margin	110 m
Turnout number	No. 18
Turnout speed	80 km/h
Distance between the train parking and exit signal	65 m
Arrival operation time (CTCS-3)	40 s
Arrival operation time (VC system)	35 s
Departure operation time (CTCS-3)	51 s
Departure operation time (VC system)	46 s
Passing operation time (CTCS-3)	25 s
Passing operation time (VC system)	20 s

and changes dynamically with the preceding train. Here, we make this assumption to simplify the calculation. For the train arrival case under CTCS-3, the approaching time equals the time needed to cross the braking distance from the full speed (i.e., 300 km/h) to station allowable speed (i.e., 80 km/h).

Outcomes for scenario 3 are shown in Table 7. I_{C-3} and I_{VC} represent train headway time under CTCS-3 and VC system, while D_{C-3} and D_{VC} represent the required distance between adjacent trains. It is worth noting that adjacent target tracks (e.g., tracks 1 and 2) usually have more associated turnouts, but the situation is the opposite for the long-distant tracks (e.g., tracks 1 and 19). According to the interval of target tracks, 20 track combinations are selected and divided into 4 sets, namely, A, B, C, and D. Set A represents the combinations of adjacent tracks (i.e., tracks are used in sequence) and set B represents the combination of two tracks that are farther apart, followed by set C and set D.

We find that the train headway under VC is greatly reduced versus that under CTCS-3. The average train headway time decreases from 204 s to 110 s, with a reduction of 46%. The average distance between two arriving trains decreases from 7936 m to 2445 m and is reduced by 69%. This proves that trains with VC conditions can perform stopping service at smaller intervals than under CTCS-3 operation, which will greatly improve the efficiency of train receiving at stations. For the train headway under CTCS-3 and VC system, the arrival operation time accounted for 19.6% and 31.8% of the total time, respectively. Hence, the arrival operation time has a great impact on VC operation and should be further optimized by shortening the system update time. Figure 12 depicts the calculation results in the form of a histogram, where the train headway time under VC and CTCS-3 is displayed in blue bars filled with diagonal lines and solid orange bars, respectively.

Table 7: Outcomes of train headways and distance in scenario 3.

No.	Set	Track G1	Track G3	Critical track elements	$I_{C-3}[s]$	$D_{C-3}[m]$	$I_{VC}[s]$	$D_{VC}[m]$
1		1	2	101/103, 109/111, 121/123 137, 157, 165	228	7537	134	2157
2		2	3	101/103, 109/111, 121/123 137, 157	219	7376	125	1996
3	A	3	4	101/103, 109/111, 121/123	223	7462	129	2082
4		4	5	101/103, 109/111, 121/123 139/141, 159, 167	228	7545	134	2165
5		5	6	101/103, 109/111, 121/123 139/141, 159	220	7384	126	2004
6		1	3	101/103, 109/111, 121/123 137, 157	219	7376	125	1996
7		3	5	101/103, 109/111, 121/123	223	7462	129	2082
8	B	5	7	101/103, 109/111, 121/123 139/141	197	6872	103	1492
9		7	11	101/103, 109/111	189	6701	95	1321
10		11	13	101/103, 117/119, 129/131 147/149, 161	222	7428	128	2048
11		1	13	101/103, 109/111	189	6701	95	1321
12		13	3	101/103, 109/111	194	6805	100	1425
13	C	3	11	101/103, 109/111	189	6701	95	1321
14		11	5	101/103, 109/111	194	6805	100	1425
15		5	7	101/103, 109/111, 121/123 139/141	197	6872	103	1492
16		1	14	101/103, 109/111	189	6701	95	1321
17		14	2	101/103, 109/111	194	6805	100	1425
18	D	2	13	101/103, 109/111	189	6701	95	1321
19		13	3	101/103, 109/111	194	6805	100	1425
20		3	12	101/103, 109/111	189	6701	95	1321

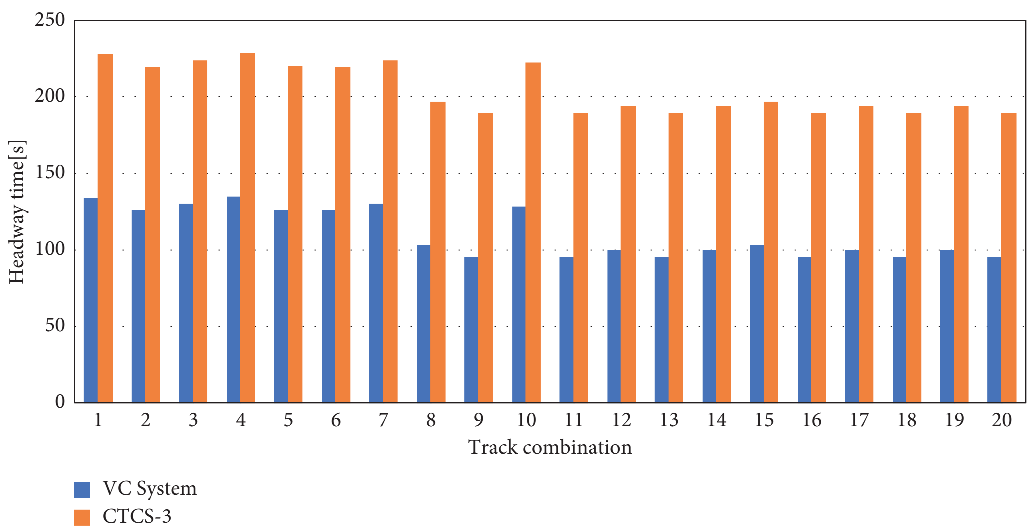

Figure 12: Outcomes of train headways for scenario 3.

We find that the train headways under the 4 track combination sets are different. For the VC system, the average headways corresponding to sets A, B, C, and D are 130 s, 116 s, 98 s, and 97 s, respectively. When referred to CTCS-3, these outcomes ranked as follows: 224 s, 210 s, 192 s, and 191 s. Therefore, the average train headway in set A displays a maximum value and is followed by B, C, and D for both systems. Set A represents track combinations with the most associated turnouts. Therefore, it will take much more time for the preceding train to clear the critical route. For these four sets under both systems, the difference between the longest train headway (corresponding to set A) and the shortest train headway (corresponding to set D) is 33 s. This indicates that either for VC or CTCS-3, track-usage sequences have an impact on train headways due to different route lengths. Moreover, based on the VC principle, train position and movement information of the preceding train should be transferred to the rear constantly to ensure safe operation. Hence, to integrate VC operation into station dispatching, accurate route information and dynamic train motion states must be taken into account when compiling operation schedules at stations.

6.2.2. Time Headway in Train Departure Case. Under the CTCS-3 principle, after the preceding train has completely cleared the first exit block section, the rear can depart. Hence, for the train departure case under CTCS-3, the train

Table 8: Outcomes of train headways for scenario 6.

No.	Set	Track G1	Track G3	Critical track elements	$I_{C-3}\,[s]$	$D_{C-3}\,[m]$	$I_{VC}\,[s]$	$D_{VC}\,[m]$
1	A	1	2	165	195	3943	103	1648
2		2	3	165, 157	195	3943	114	1907
3		3	4	157, 137	191	3868	111	1832
4		4	5	167	195	3951	103	1648
5		5	6	167, 159	195	3951	110	1821
6	B	1	3	165, 157	195	3862	114	1907
7		3	5	157, 137	191	3998	122	2077
8		5	7	167, 159, 139/141, 137 121/123	195	3998	129	2234
9		11	13	171, 161	196	3965	113	1885
10		13	15	173, 161, 147/149, 151/153 125/127	195	3965	129	2247
11		15	17	175, 151/153, 155	196	3961	122	2084
12	C	1	4	165, 157, 137	195	3961	114	1907
13		4	7	167, 159, 139/141, 137 121/123	195	3967	129	2234
14		11	15	171, 161, 147/149, 151/153 125/127	196	3967	131	2281
15		15	18	175, 151/153, 155	196	3921	122	2084
16	D	1	19	165, 157, 137, 121/123, 109/111, 101/103	195	3921	145	2587
17		19	2	135, 133, 125/127, 113/115 101/103	180	3607	130	2251
18		2	18	165, 157, 137, 121/123, 109/111, 101/103	195	3943	145	2587
19		18	3	163, 155, 133, 125/127 113/115, 101/103	194	3943	144	2565
20		3	17	157, 137, 121/123, 109/111 101/103	191	3868	141	2512

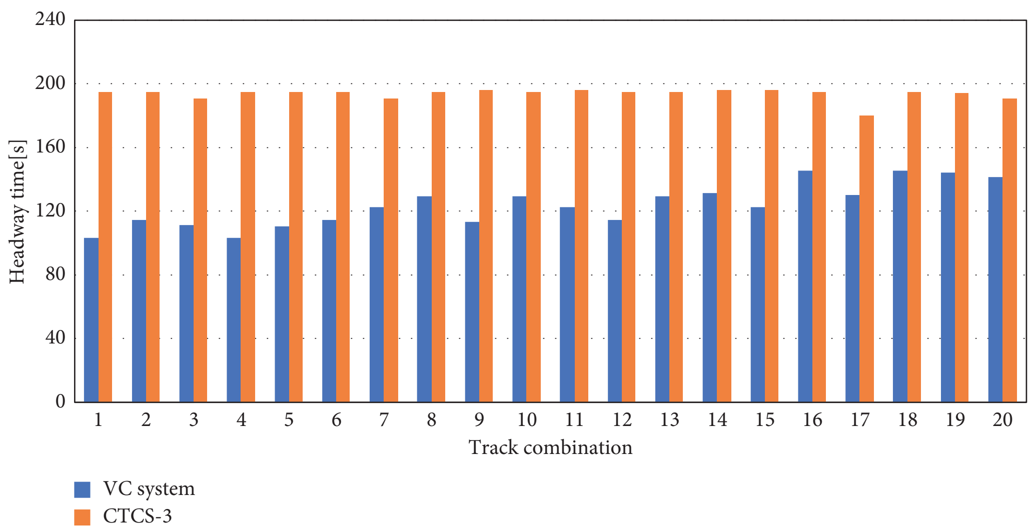

Figure 13: Outcomes of train headways for scenario 6.

headway is only affected by the length of the exit route that the preceding train needs to traverse and is not affected by the usage of track sequences. Representative track combinations are selected to carry out computations for VC system, i.e., sets A, B, C, and D. Outcomes for scenario 6 under VC system (I_{VC}) and CTCS-3 (I_{C-3}) are shown in Table 8.

For the departing case described in scenario 6, train headway under VC is much shorter than that under CTC3-3. The average train headway time decreases from 194 s to 124 s with a reduction of 36%, while the distance interval decreases from 3925 m to 2115 m and is reduced by 46%. Trains under VC operation can depart at smaller time intervals and, subsequently, form a convoy on the run. Therefore, the reduction of departing headway is also crucial to determine whether VC can bring sufficient capacity gains for a railway corridor. Like the train arrival case, the train departure operation time accounts for 37% of the total train headway time and should be further optimized by improving system performance. Figure 13 depicts outcomes for scenario 6; blue and orange bars respectively report train headways under VC system and CTCS-3.

The train headway is concerned with the critical track elements under the VC system, and the average headways corresponding to track combination sets A, B, C, and D are 108 s, 122 s, 125 s, and 141 s, respectively. Set A represents track combinations with the most associated switches. Therefore, the preceding train can enter the common route

Table 9: Outcomes of train headways in scenario 5.

No.	Set	Track G1	Track G3	Critical track elements	$I_{C-3}\,[s]$	$I_{VC}\,[s]$
1	A	1	2	101/103, 109/111, 121/123 137, 157, 165	176	116
2		2	3	101/103, 109/111, 121/123 137, 157	168	108
3		3	4	101/103, 109/111, 121/123	173	112
4		4	5	101/103, 109/111, 121/123 139/141, 159, 167	177	117
5		5	6	101/103, 109/111, 121/123 139/141, 159	169	109
6	B	1	3	101/103, 109/111, 121/123 137, 157	169	108
7		3	5	101/103, 109/111, 121/123	173	112
8		5	7	101/103, 109/111, 121/123 139/141	146	86
9		7	11	101/103, 109/111	139	78
10		11	13	101/103, 117/119, 129/131 147/149, 161	172	111
11	C	1	13	101/103, 109/111	139	78
12		13	3	101/103, 109/111	144	83
13		3	11	101/103, 109/111	140	78
14		11	5	101/103, 109/111	144	83
15		5	7	101/103, 109/111, 121/123 139/141	148	86
16	D	1	14	101/103, 109/111	140	78
17		14	2	101/103, 109/111	145	83
18		2	13	101/103, 109/111	140	78
19		13	3	101/103, 109/111	145	83
20		3	12	101/103, 109/111	141	78

Table 10: Outcomes of train headways in scenario 8.

No.	Set	Track G1	Track G3	Critical track elements	$I_{C-3}\,[s]$	$I_{VC}\,[s]$
1	A	1	2	165	287	241
2		2	3	165, 157	287	247
3		3	4	157, 137	293	244
4		4	5	167	287	236
5		5	6	167, 159	287	243
6	B	1	3	165, 157	287	247
7		3	5	157, 137	283	255
8		5	7	167, 159, 139/141, 137 121/123	287	262
9		11	13	171, 161	288	246
10		13	15	173, 161, 147/149, 151/153 125/127	287	263
11		15	17	175, 151/153, 155	288	255
12	C	1	4	165, 157, 137	287	247
13		4	7	167, 159, 139/141, 137 121/123	287	262
14		11	15	171, 161, 147/149, 151/153 125/127	288	264
15		15	18	175, 151/153, 155	288	255
16	D	1	19	165, 157, 137, 121/123, 109/111, 101/103	287	278
17		19	2	135, 133, 125/127, 113/115 101/103	272	263
18		2	18	165, 157, 137, 121/123, 109/111, 101/103	287	278
19		18	3	163, 155, 133, 125/127 113/115, 101/103	286	277
20		3	17	157, 137, 121/123, 109/111 101/103	283	274

earlier under the track combinations involved in set A than others, i.e., the track combinations involved in sets B, C, and D. For these four sets, the difference between the longest (corresponding to set D) and shortest (corresponding to set A) train headways is 33 s. Therefore, the sequence of track usage also has a considerable effect on the train headway in train departure cases.

Moreover, we find that for both systems, the train headway in scenario 6 is shorter than that in scenario 3. This indicates that the train arrival case is more restrictive than the train departure case for station capacity.

7. Conclusion

This paper introduces an advanced signalling technology named virtual coupling as well as a structure of VC system based on CTCS-4 specifications. The calculation principles of train headways corresponding to the MBS and VC system are compared with the conventional blocking time model for FBS. Typical train-following operational scenarios are selected to better study the characteristics of train separation under VC operations, among which station-related scenarios are emphasized as they are critical for high-speed railways to achieve virtual coupling/decoupling manoeuvre. A multiscenario-based train headway analysis is proposed to elaborate the computation principles of train headways under VC signalling, which comprehensively considers the station configurations (e.g., track elements, train route, and signals) and technological characteristics (e.g., V2V communication layer and onboard ATO) of VC system. The train headway calculation model has been applied to Shanghai-Hongqiao Station on the Beijing-Shanghai high-speed railway to carry out theoretical computations. Two typical scenarios (i.e., trains arriving at a station and trains departing from a station) are highlighted, and outcomes corresponding to VC system and CTCS-3 are proposed as a comparative analysis to identify headways compressions brought by VC.

The results show that train headways in the train arrival case and train departure case are significantly reduced by VC, with reductions of 46% and 36% versus CTCS-3. The number of receiving and departing trains is increased if decoupling and coupling operations can be initiated at stations. We also demonstrate that the station infrastructure layout and track occupancy sequences have effects on train headways. For train arrival cases, the less critical track elements will lead to shorter train headways. In the case of a train departure, the earlier the preceding train enters the common route, the shorter the corresponding train headway. Therefore, due to the high requirements for the safety and reliability of VC, critical track elements should be considered in dispatching trains at stations.

It should be noted that some specific parameters used in our case study need to be modified by further experiments. The proposed computational method of train headways can be improved by considering trains with different motion parameters. An accurate and practical simulation model is crucial to obtain dynamic train headways under VC. In addition, the junction-related scenarios (i.e., trains dynamically coupling/decoupling at merging/diverging junctions) have great potential and are worth investigating for other railway markets in future research.

Appendix

A. Train Dynamic Motion Model

The forces on a train consist of traction/braking force and resistance. The tractive/braking force depend on the technical conditions of trains, and the resistance is composed of basic resistance and additional resistance. The basic resistance generated by several types of friction and aerodynamic resistance always exists during operations. When the train is running in special circumstances such as tunnels, ramps, and curves, additional resistance should be added. Generally, stations of high-speed railways are located in flat areas. The additional resistance can hence be ignored when calculating train motions (e.g., speed, distance, and acceleration) in station-related scenarios.

The basic resistance can be expressed as follows:

$$W_0 = m + nv + kv^2, \tag{A.1}$$

where W_0 is the basic resistance unit, N/kN; v is the train speed, m/s; m, n, k are empirical parameters related to the basic resistance.

Hence, if the tractive acceleration or braking deceleration at different speed levels is specified, the train acceleration can be expressed as

$$a = a_1(v) - a_0(v) = a_1(v) - \frac{W_0 \times g}{1000}, \tag{A.2}$$

where $a_1(v)$ is the tractive acceleration or braking deceleration at speed; $a_0(v)$ is the basic resistance deceleration, m/s^2; g is the gravitational acceleration with a value of 9.81 N/Kg.

Since the acceleration changes continuously with the movement of the train, we divide the train speed into small intervals, and the train movement corresponding to each interval can be regarded as uniform acceleration. In the speed range Δv, given the initial speed v_0, the final speed v can be expressed as

$$v = v_0 \pm \Delta v. \tag{A.3}$$

The average speed v_p in the speed range Δv is expressed as

$$v_p = \frac{v_0 + v}{2}. \tag{A.4}$$

Hence, the acceleration a in the speed range Δv can be rewritten as

$$a = a_1(v_p) - \frac{\left(m + nv_p + kv_p^2\right) \times g}{1000}. \tag{A.5}$$

The train running distance Δs and time Δt corresponding to the speed range Δv can be obtained:

$$\Delta s = \frac{(v/3.6)^2 - (v_0/3.6)^2}{2a} \quad \Delta t = \frac{\Delta s}{v_p/3.6}. \tag{A.6}$$

The distance s and time t in a larger speed range can be obtained by adding up the Δs and Δt corresponding to each Δv:

$$s = \sum \Delta s \quad t = \sum \Delta t. \tag{A.7}$$

B. Train Headways in Other Station-Related Scenarios

Scenario 1 refers to the case in which a convoy runs on the main line, and each train is controlled by the cooperative driving strategy. When a convoy passes through a station (scenario 2), trains can consecutively pass like running on the main line. The focus of the study is to investigate the train-following manoeuvres in station-related scenarios and analyze how VC affects the train headways. Therefore, the train headways of other station-related scenarios (i.e., scenarios 4, 5, 7, and 8) have been calculated and the outcomings are reported in this appendix.

Based on the train headway calculation method specified in Section 5.2, we carry out the train headway computations for CTCS-3 and VC for scenarios 4, 5, 7, and 8. In scenario 4, the preceding train passes through the station at 300 km/h and the rear needs to stop. For CTCS-3 and VC cases, the approaching time and the time for train arriving operation (i.e., 40 s for the CTCS-3 case and 35 s for the VC case) are the same as those in scenario 3. The route of the preceding train occupying the station is unique (i.e., from the home signal to the opposite exit signal on the main track). While the train headway under CTCS-3 is 168 s, it is 74 s under VC, with a reduction of 56%.

In scenario 5, the preceding train stops and the rear passes through the station. For VC and CTCS-3 cases, the times for clearing the critical elements are the same as those in scenario 3. For the CTCS-3 case, the train approaching time equals the time for the rear train to cross the absolute braking distance (i.e., distance needed to decelerate from 300 km/h to 80km/h). For the VC case, the train approaching time is the time for the rear train to cross the absolute braking distance (i.e., distance needed to decelerate from 80 km/h to zero) at its original speed 300 km/h. In addition, the train passing operation time under CTCS-3 is set to 25 s, and that under VC is 20 s. The train headway results of scenario 5 are represented in Table 9. The average train headway corresponding to scenario 5 under CTCS-3 is 154 s, and it is 93 s under VC, which is reduced by 40%.

In scenario 7, the preceding train passes through the station and the rear departs. The times needed for train departure operations are the same as those in scenario 6 (i.e., 51 s for the CTCS-3 case and 46 s for the VC case). The route of the preceding train occupying the station is unique. For CTCS-3, the preceding train travels from the exit signal to the end of the first exit block section at 300 km/h. For VC, the preceding train travels from the exit signal to the opposite home signal at 300 km/h. The corresponding train headway under CTCS-3 is 81 s, while it is 63 s under VC, with a reduction of 22%.

In scenario 8, the preceding train departs and the rear passes through the station. For the sake of safety, the preceding train must accelerate to the speed of the rear train under CTCS-3 and VC cases. Therefore, after the preceding train clears the opposite home signal (VC case) or the first exit block section (CTCS-3 case), it needs to continue to accelerate to reach 300 km/h. The train headway results of scenario 8 are represented in Table 10.

The average train headway of scenario 8 under CTCS-3 is 286 s, and it is 257 s under VC, which is reduced by 10%. We can find that the benefit brought by VC is not significant due to the additional acceleration time for both VC and CTCS-3 cases. It is unfavourable for the implementation of virtual coupling if the train headway is too long during the departure process. Therefore, the rear train can slow down a bit earlier so that the preceding train can reach the rear train's speed as soon as possible.

Data Availability

Some or all data, models, or codes that support the findings of this study are available from the corresponding author upon reasonable request.

Conflicts of Interest

The authors declare that there are no conflicts of interest regarding the publication of this paper.

Acknowledgments

This research was supported by the National Natural Science Foundation of China (Nos. U1834209 and 71701174).

References

[1] S. Zhan, S. C. Wong, and S. M. Lo, "Social equity-based timetabling and ticket pricing for high-speed railways," *Transportation Research Part A: Policy and Practice*, vol. 137, pp. 165–186, 2020.

[2] I. Hansen, *Railway Timetable Traffic: Analysis, Modelling, Simulation*, Eurailpress, no. 1, Hamburg, 2008.

[3] C. Tian, S. Zhang, Y. Zhang, and X. Jiang, "Study on the train headway on automatic sections of high-speed railway," *Journal of the China Railway Society*, vol. 37, no. 10, pp. 1–6, 2015.

[4] L. Hou, P. Sun, Y. Nie, and Q. Wang, "A study on optimizing high-speed railway tracking intervals," *Railway Transportation and Economy*, vol. 40, no. 6, pp. 5–11, 2018.

[5] M. Haltuf, "Shift2Rail JU from member state's point of view," *Transportation Research Procedia*, vol. 14, pp. 1819–1828, 2016.

[6] Shift2Rail, "The rail joint undertaking," 2019.

[7] I. Mitchell, "ERTMS level 4, train convoys or virtual coupling," *Intelligent Technology Committee*, vol. 219, pp. 1–3, 2016.

[8] E. Quaglietta, M. Wang, and R. M. P. Goverde, "A multi-state train-following model for the analysis of virtual coupling railway operations," *Journal of Rail Transport Planning and Management*, vol. 15, 2020.

[9] X2Rail-1, "The rail joint undertaking," 2015, https://shift2rail.org/x2rail/.

[10] Roll2Rail, "The rail joint undertaking," 2015, http://www.roll2rail.eu/.

[11] In2Rail, "The rail joint undertaking," 2015, http://www.in2rail.eu/home.aspx.

[12] MovingRail, *Deliverable D4.2, Cost-Effectiveness Analysis for Virtual Coupling*, Shift2Rail, 2020, https://www.networkrail.co.uk/industry-and-commercial/research-development-and-technology/research-and-development-programme/shift2rail/.

[13] T. Schumann, "Increase of capacity on the shinkansen high-speed line using virtual coupling," *International Journal of Transport Development and Integration*, vol. 1, no. 4, pp. 666–676, 2017.

[14] R. Liu, "Simulation model of speed control for the moving-block systems under ERTMS level 3," in *Proceedings of the IEEE International Conference on Intelligent Rail Transportation (ICIRT)*, pp. 322–327, Birmingham, UK, August 2016.

[15] J. Pachl, *Railway Signalling Principles*, Braunschweig, 2020.

[16] *General Rules of CTCS Technical Specification for Train Operation Control System in China (Provisional)*, Ministry of Railways of the People's Republic of China, China, Science and Technology Transport Letter No.14, 2004.

[17] X2Rail-2, *Deliverable D3.1, System Requirement Specification of the Fail-Safe Train Positioning Functional Block*, Shift2Rail, 2018.

[18] MovingRail, *Deliverable D4.1. Market Potential and Operational Scenarios for Virtual Coupling*, Shift2Rail, 2019.

[19] MovingRail, *Deliverable D3.1, Virtual Coupling Communication Solutions Analysis*, Shift2Rail, 2020.

[20] U. Bock and J. U. Varchmin, *Enhancement of the Occupancy of Railroads Using Virtually Coupled Train Formations*, World Congress on Railway Research, Tokyo, Japan, 1999.

[21] U. Bock and G. Bikker, "Design and development of a future freight train concept - "virtually coupled train formations"," *IFAC Proceedings Volumes*, vol. 33, no. 9, pp. 395–400, 2000.

[22] I. K. S. Braun and E. Schnieder, "Concepts on a future railway management system," in *Proceedings of the 8th World Congr. Intell. Transp. Syst. ITS Amer., ITS Aust., ERTICO (Intell. Transp. Syst. Services-Eur.)*, pp. 1–8, Singapore, 2001.

[23] D.-I. T. Ständer, D.-I. J. Drewes, and D.-W.-I. I. Braun, "Operational and safety concepts for railway operation with virtual train-sets," *IFAC Proc. Volumes*, vol. 39, no. 12, pp. 261–266, 2006.

[24] J. Goikoetxea, "Roadmap towards the wireless virtual coupling of trains," *Lecture Notes in Computer Science*, in *Proceedings of the Int. Workshop Communication Technologies for Vehicles*, pp. 3–9, San Sebastian, Spain, July 2016.

[25] S. Zhan, S. C. Wong, P. Shang, Q. Peng, J. Xie, and S. M. Lo, "Integrated railway timetable rescheduling and dynamic passenger routing during a complete blockage," *Transportation Research Part B: Methodological*, vol. 143, pp. 86–123, 2021.

[26] D. Pan, Y. Zheng, and C. Zhang, "On intelligent automatic train control of railway moving automatic block systems based on multi-agent systems," in *Proceedings of the 29th Chinese Control Conference*, pp. 4471–4476, Beijing, China, July 2010.

[27] B. Ning, H. Dong, S. Gao, T. Tang, and W. Zheng, "Distributed cooperative control of multiple high-speed trains under a moving block system by nonlinear mapping-based feedback," *Science China Information Sciences*, vol. 61, pp. 1–12, 2018.

[28] S. Gao, H. Dong, B. Ning, and Q. Zhang, "Cooperative prescribed performance tracking control for multiple high-speed trains in moving block signaling system," *IEEE Transactions on Intelligent Transportation Systems*, vol. 20, no. 7, pp. 2740–2749, 2019.

[29] C. Di Meo, M. Di Vaio, F. Flammini, R. Nardone, S. Santini, and V. Vittorini, "ERTMS/ETCS virtual coupling: proof of concept and numerical analysis," *IEEE Transactions on Intelligent Transportation Systems*, vol. 21, no. 6, pp. 2545–2556, 2020.

[30] L. Liu, P. Wang, B. Zhang, and W. Wei, "Coordinated control method of virtually coupled train formation based on multi agent systems," in *Proceedings of the The Second International Conference on Smart Vehicular Technology, Transportation, Communication and Applications*, Chengdu, China, May 2018.

[31] H. Liu, H. Yang, and B. Cai, "Optimization for the following operation of a high-speed train under the moving block system," *IEEE Transactions on Intelligent Transportation Systems*, vol. 19, no. 10, pp. 3406–3413, 2018.

[32] J. Felez, Y. Kim, and F. Borrelli, "A model predictive control approach for virtual coupling in railways," *IEEE Transactions on Intelligent Transportation Systems*, vol. 20, no. 7, pp. 2728–2739, 2019.

[33] L. Liu, P. Wang, Y. Wang, W. Wei, and Z. Wang, "Dynamic train formation and dispatching for rail transit based on virtually coupled train set," in *Proceedings of the IEEE Intelligent Transportation Systems Conference (ITSC)*, pp. 2823–2828, Auckland, New Zealand, October 2019.

[34] J. Aoun, E. Quaglietta, and R. M. P. Goverde, "Investigating market potentials and operational scenarios of virtual coupling railway signaling," *Transportation Research Record: Journal of the Transportation Research Board*, vol. 2674, no. 8, pp. 799–812, 2020.

[35] *Next Generation Train on the DLR Homepage*, http://www.dlr.de/dlr/en/desktopdefault.aspx/tabid- 10467/740_read-916/#/gallery/2043, 2016.

[36] M. Mei, Z. Chen, D. Pan, and D. Yuan, "Analysis and calculation of train departure time in the same direction at a station under the condition of moving block," *Control and Information Technology*, pp. 71–75, 2019.

[37] L. Liu, P. Wang, W. Wei, Q. Li, and B. Zhang, "Intelligent dispatching and coordinated control method at railway stations for virtually coupled train sets," in *Proceedings of the 2019 IEEE Intelligent Transportation Systems Conference (ITSC)*, pp. 607–612, Auckland, New Zealand, October 2019.

[38] I. Hansen and J. Pachl, Eds., *Railway Timetabling & Operations – Analysis, Modelling, Optimisation, Simulation, Performance Evaluation*, Eurail Press, Hamburg, 2014.

[39] E. Quaglietta, "Analysis of Platooning Train Operations under V2V communication-based signalling: fundamental modelling and capacity impacts of Virtual Coupling," in *Proceedings of the 98th Transportation Research Board Annual Meeting*, Washington DC, January 2019.

[40] G. J. L. Naus, R. P. A. Vugts, J. Ploeg, and J. G. MArinus, "String-stable cacc design and experimental validation: a frequency-domain approach," *IEEE Transactions on Vehicular Technology*, vol. 59, no. 9, pp. 4268–4279, 2010.

[41] R. Rajamani and C. Zhu, "Semi-autonomous adaptive cruise control systems," in *Proceedings of the 1999 American Control Conference (Cat. No. 99CH36251)*, vol. 2, pp. 1491–1495, San Diego, CA, USA, June 1999.

[42] G. Ma, *Rail Transportation Vehicle and Train Traction Calculation*, Southwest Jiaotong University, Chengdu, 2011.